Proceedings of the International Symposium on Engineering Lessons Learned from
the 2011 Great East Japan Earthquake, March 1-4, 2012, Tokyo, Japan

ESTIMATION OF STRONG MOTION DURING THE 2011 OFF THE PACIFIC COAST OF TOHOKU EARTHQUAKE BY A GROUND MOTION PREDICTION MODEL

KATAOKA Shojiro[1] and KANEKO Masahiro[2]

[1] Senior Researcher, Earthquake Disaster Prevention Division, National Institute for Land and Infrastructure Management, Tsukuba, Japan, kataoka-s92rc@nilim.go.jp
[2] Head, Earthquake Disaster Prevention Division, National Institute for Land and Infrastructure Management, Tsukuba, Japan, kaneko-m92pq@nilim.go.jp

ABSTRACT: A Ground motion prediction model that was derived prior to the 2011 off the Pacific coast of Tohoku earthquake is applied to simulation of ground motion during the giant earthquake. Saturation of ground motion intensity with magnitude is investigated using the observed records and estimated ground motion during hypothetical Suruga-Nankai trough earthquakes by the Central Disaster Prevention Council. The simulated waveforms and observed records are compared and discussed.

Key Words: the 2011 off the Pacific coast of Tohoku earthquake, ground motion prediction equation, acceleration response spectrum, group delay time

INTRODUCTION

Empirical equations for ground motion, or ground motion prediction equations (GMPEs), are still one of the reliable methods for ground motion prediction among others such as semi-empirical methods and theoretical methods. New empirical equations for acceleration response spectrum and group delay time that enable prediction of time history waveform of ground motion were developed prior to the 2011 off the Pacific coast of Tohoku earthquake. This paper presents the results of estimation of strong motion during the M_w9.0 earthquake and examines applicability of the GMPEs to giant earthquakes.

GROUND MOTION PREDICTION EQUATION

GMPE for acceleration response spectrum

Fig. 1 shows 29 earthquakes, which are not crustal earthquakes, and 1,609 strong motion stations of which strong motion records were used for the following regression analyses. The largest earthquake among them is the 2003 off Tokachi earthquake (moment magnitude M_w8.2, No. 7 in Fig. 1). The

total of 7,592 records was used; these records were obtained by Japan Meteorological Agency (JMA) and National Research Institute for Earth Science and Disaster Prevention (K-NET and KiK-net). Distance-moment magnitude relationship of the strong motion records is shown in Fig. 2.

The following model was employed for the regression analysis for acceleration response spectrum.

$$\log S_A(T) = a_1(T)\, M_w + a_2(T)\, D - \log(X^{d(T)} + p(T)10^{qMw}) - b(T)\, X + c_0(T) + c_j(T) \qquad (1)$$

where S_A is acceleration response spectrum [cm/s^2] (critical damping ratio h=0.05), T is natural period [s], D is focal depth [km], X is distance to source fault [km], a_1, a_2, b, c_0, d, p, and q are regression coefficients, and c_j is correction coefficient for station j.

The two-step regression analysis (Kataoka *et al.*, 2008) was employed. The coefficients a_1, a_2, b, and c_0 derived by the regression analysis are shown in Fig. 3. Coefficient d was found to be 1.0 throughout the target period range, T = 0.1-10[s], and q was set to 0.4.

GMPE for group delay time

The following models were employed for the regression analysis for average and variance of group delay time. Eq. (2) is the same as the model of Satoh *et al.* (2010), while Eq. (3) is different for R is used in Satoh *et al.* (2010) instead of R^2.

$$\mu(T) = a(T)\, M_0^{1/3} + b(T)\, R + c_j(T) \qquad (2)$$

$$\sigma^2(T) = a(T)\, M_0^{1/3} + b(T)\, R^2 + c_j(T) \qquad (3)$$

where μ and σ^2 are average [s] and variance [s^2] of group delay time, M_0 is seismic moment [N·m], T is period [s], R is hypocentral distance [km], a and b are regression coefficients, and c_j is correction coefficient for station j. The coefficients a and b derived by the regression analysis are shown in Figs. 4 and 5.

The combination of GMPEs for acceleration response spectrum and group delay time enables to estimate time history waveform of ground motion (Satoh *et al.*, 2010).

SATURATION OF GROUND MOTION INTENSITY WITH MAGNITUDE

Fig. 6 compares $S_A(T$=1[s]) of observed ground motion with the GMPE derived above. Two kinds of observed S_A (T=1[s]) are plotted in Fig. 6; original ones and corrected (site amplification characteristics are removed by c_j) ones. It can be seen that the GMPE overestimate the ground motion when M_w is set to 9.0. The GMPE was found to have least misfit with the corrected S_A (T=1[s]) when M_w was set to 8.3. Fig. 7 summarizes the moment magnitudes that give the GMPE the least misfit with the corrected S_A (T = 0.1-10[s]).

In order to investigate how $S_A(T)$ varies with M_w in the range of M_w>8.0, ground motions during hypothetical Tokai, Tonankai, and Nankai earthquakes (M_w8.0, 8.2, and 8.4) and their coupled earthquakes (M_w8.3-8.7) that had been estimated by the Central Disaster Prevention Council in 2002 were stochastically analyzed. As shown is Fig. 8, $S_A(T)$ were found not to get larger with M_w any longer when the magnitude became larger than 8.2, in other words, $S_A(T)$ saturated at M_w8.2.

ESTIMATION OF GROUND MOTION BY THE GMPE

Source fault of the 2011 off the Pacific coast of Tohoku earthquake

A 3-segment source fault was set for estimation of ground motion by the GMPEs as shown in Fig. 9 based on the source model obtained from inversion of strong motions (Yoshida *et al.*, 2011). Seismic

moments were set to 6.52 x 10^{21} [N·m] (M_w8.48), 1.85 x 10^{22} [N·m] (M_w8.78), and 8.63 x 10^{21} [N·m] (M_w8.56), while rupture starting times were set to 0 [s], 40 [s], and 100 [s] (Satoh *et al.*, 2011) for segment 1, 2, and 3, respectively. Though M_w of all segments are larger than 8.5, they were set to 8.3 for estimation of $S_A(T)$ following the results of the previous chapter.

In addition to the 3-segment source fault, a single fault model was set for comparison of time history waveforms. The seismic moment of the single fault model was set to 3.36 x 10^{22} [N·m] (M_w8.95), which is equivalent to the sum of seismic moments of the 3 segments. Rupture starting point is the same as segment 1 and 2.

Comparison between observed and estimated ground motions

Figs. 10 and 11 compare the time history waveforms of the observed and the estimated ground motions. The correction coefficient obtained for each station was applied to compensate the GMPEs for site amplification and phase characteristics. The waveforms of the 3-segment model show, as a whole, an agreement with observed ones, while those of single fault model seem too simple for ground motions at stations in Miyagi prefecture, i.e. MYG006, MYGH10, Wakuya Branch, and Naruse Weir. Detailed investigations are necessary for a better agreement; several research groups have proposed even more complicated source model such as the one by Kurahashi and Irikura (2011) that consists of 5 strong motion generation areas.

Fig. 12 shows comparisons of the acceleration response spectra. The observed and estimated results don't show a very good agreement, especially at MYG006. Applicability of the site correction coefficient to giant earthquakes must be improved by taking consideration of various effects, travel path for instance, neglected in this study.

CONCLUSIONS

A Ground motion prediction model that was derived prior to the 2011 off the Pacific coast of Tohoku earthquake is applied to simulation of ground motion during the giant earthquake. Saturation of ground motion intensity with magnitude is investigated using the observed records and estimated ground motion during hypothetical Suruga-Nankai trough earthquakes by the Central Disaster Prevention Council. It was found that acceleration response spectra of both of observed and estimated ground motions saturate around M_w 8.3. The simulated waveforms and observed records are compared and discussed. Further investigation is needed for a better agreement between observed and estimated ground motions.

ACKNOWLEDGMENTS

The authors are grateful to Dr. Yasuhiro Yoshida, Meteorological Research Institute, JMA, for the detailed data of the source fault. The strong motion records obtained by National Research Institute for Earth Science and Disaster Prevention (K-NET and KiK-net), JMA, and Ministry of Land, Infrastructure, Transport and Tourism are used in this study.

REFERENCES

Kataoka, S., Matsumoto, S., Kusakabe, T. and Toyama, N. (2008). "Attenuation relationships and amplification map for ground motion in rather-long period range, *Proceedings of Japan Society for Civil Engineers* A, Vol. 64, No. 4, 721-738.

Kurahashi, S. and Irikura, K. (2011). "Source model for generating strong ground motions during the 2011 off the Pacific coast of Tohoku Earthquake", *Earth Planets Space*, Vol. 63, 571-576.

Satoh, T., Okawa, I., Nishikawa, T., Sato, T. and Seki, M. (2010). "Prediction of waveforms of long-period ground motions for hypothetical earthquakes using empirical regression relations of response spectra and phase spectra, *Journal of Structural and Construction Engineering* (Transactions of AIJ), Vol. 75, No. 649, 521-530.

Satoh, T., Okawa, I., Nishikawa, T., and Sato, T. (2011). "Simulation of long-period ground motions during the 2011 off the Pacific coast of Tohoku earthquake using empirical regression relations, *Proceeding of the 8th Annual Meeting of Japan Association for Earthquake Engineering*, 430-431.

Yoshida, Y., Ueno, H., Muto, D., and Aoki, S. (2011). "Source process of the 2011 off the Pacific coast of Tohoku Earthquake with the combination of teleseismic and strong motion data." *Earth Planets Space*, Vol. 63, 565-569.

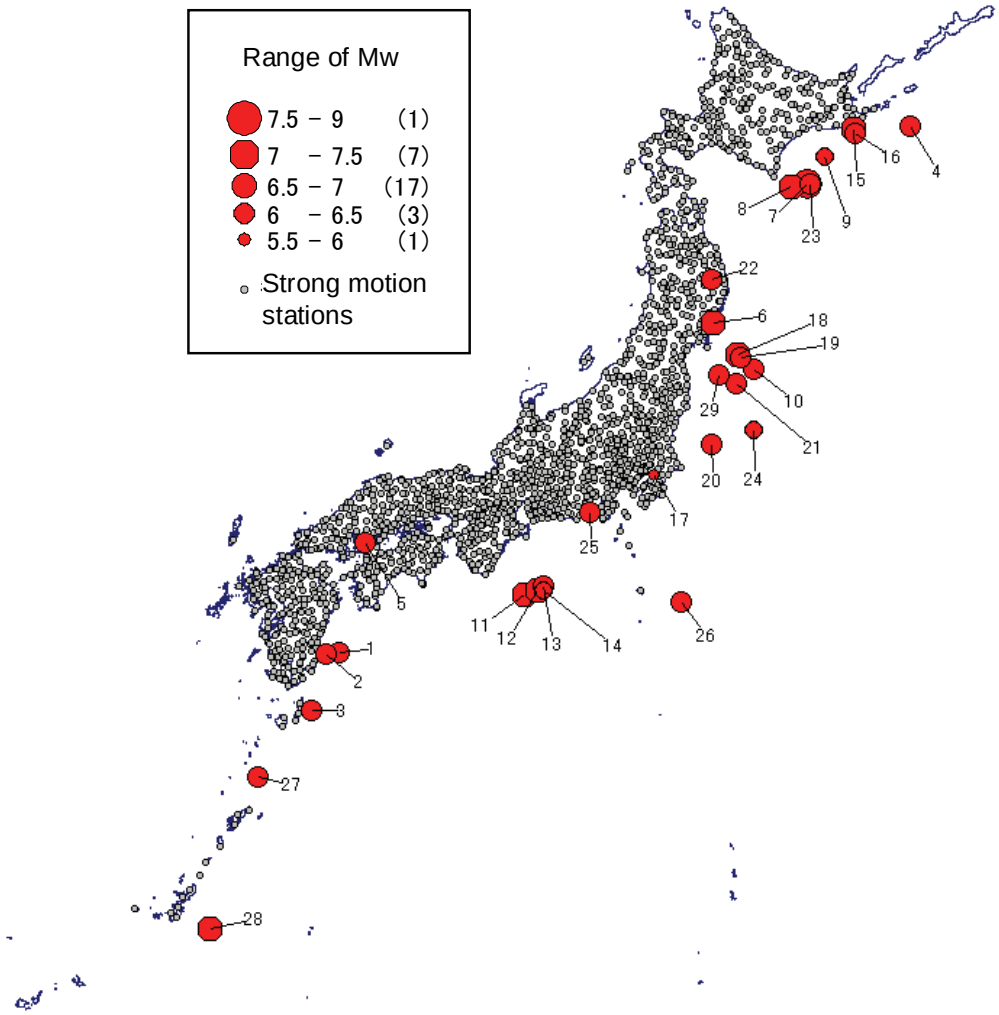

Fig. 1 Epicenters of 29 earthquakes and 1609 strong motion stations of which strong motion records were used for the regression analyses in this study.

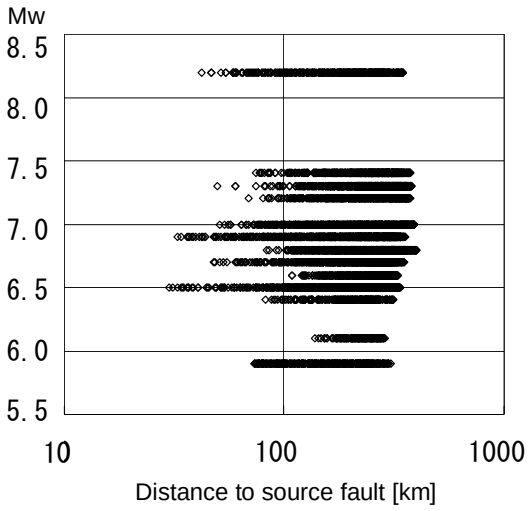

Fig. 2 Distance-moment magnitude relationship of the strong motion records used in this study.

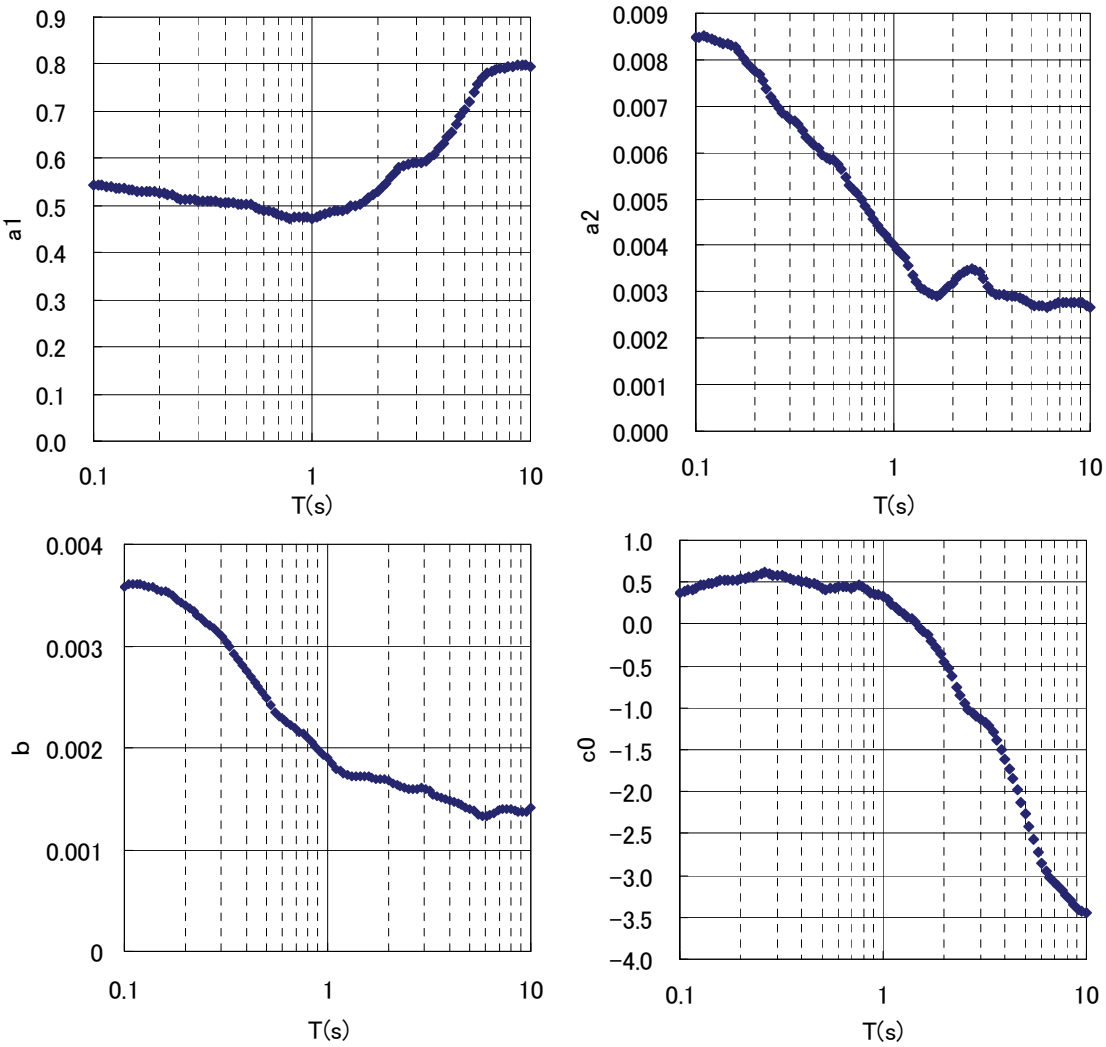

Fig. 3 Coefficients a_1, a_2, b, and c_0 derived from the regression analysis for acceleration response spectra.

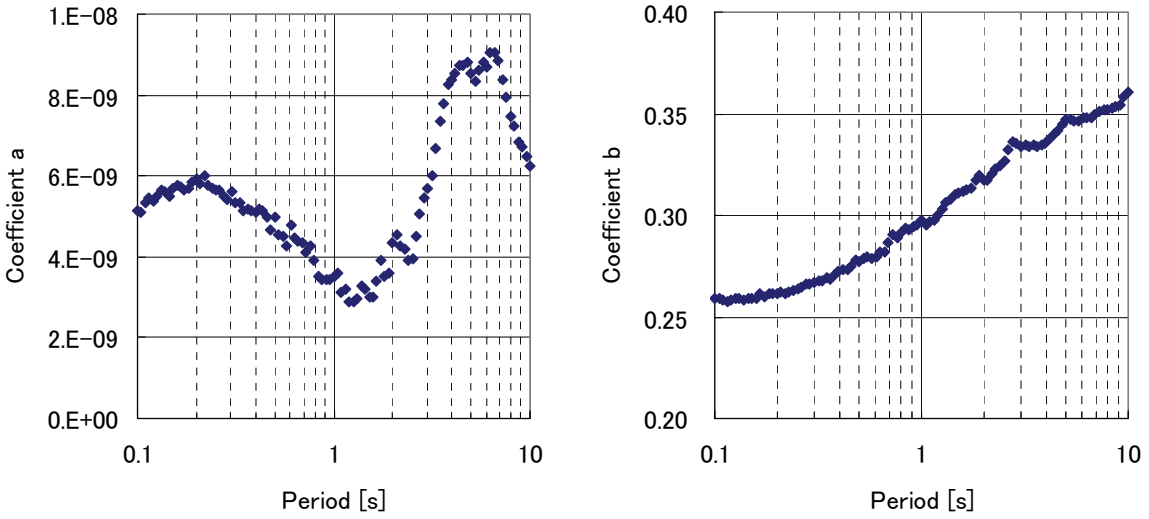

Fig. 4 Coefficients *a* and *b* derived from the regression analysis for average group delay time, μ.

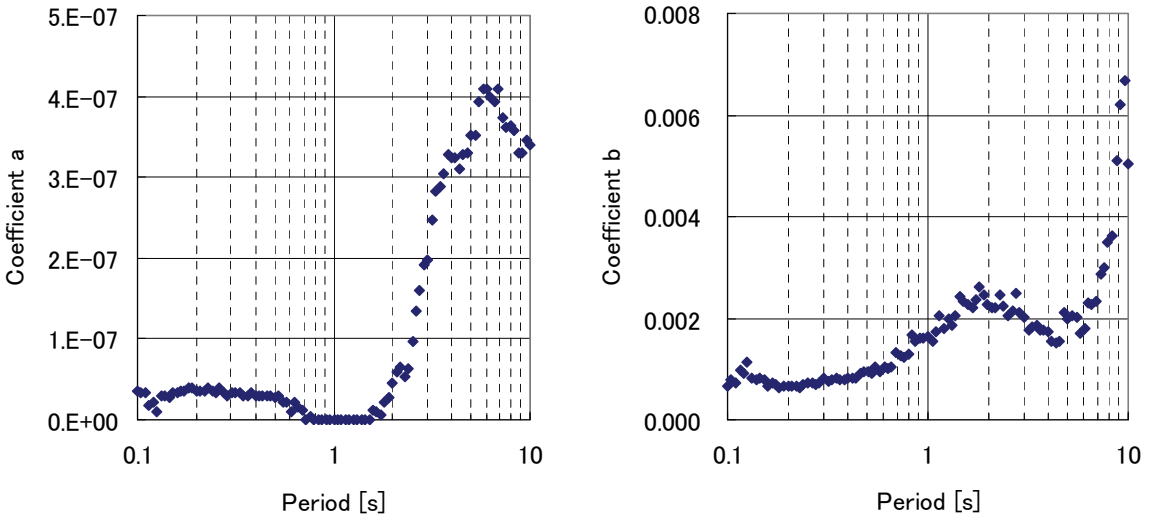

Fig. 5 Coefficients *a* and *b* derived from the regression analysis for variance of group delay time, σ^2.

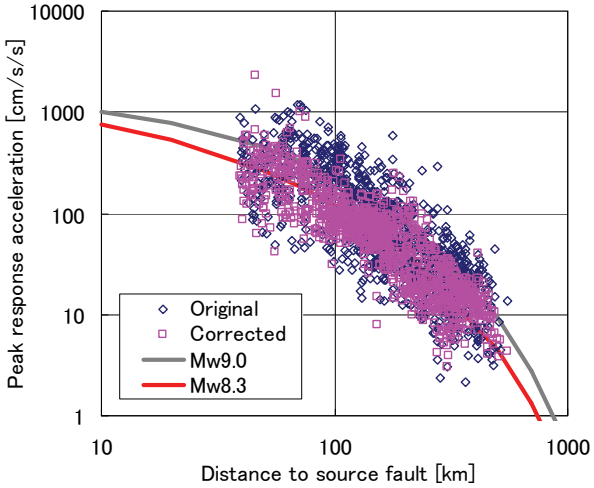

Fig.6 Observed and corrected strong motion ($S_A(T = 1[s])$) compared with the GMPE. The GMPE gives the least misfit with the observed $S_A(T = 1[s])$ when M_w is set to 8.3.

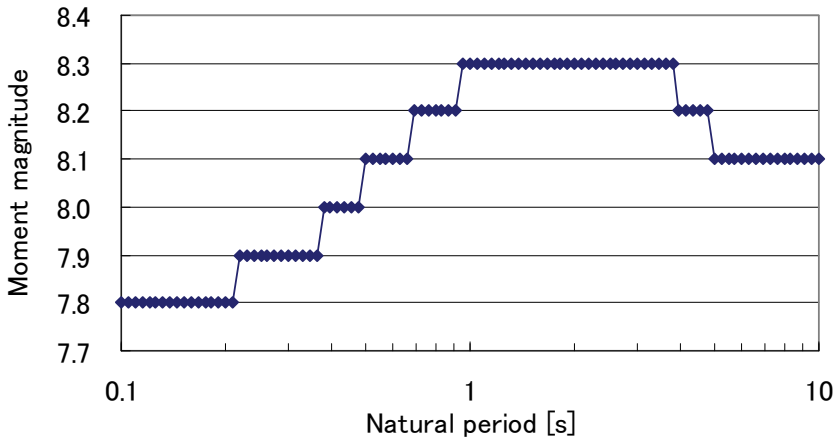

Fig. 7 Moment magnitude that gives the GMPE for $S_A(T)$ the least misfit with observed $S_A(T)$.

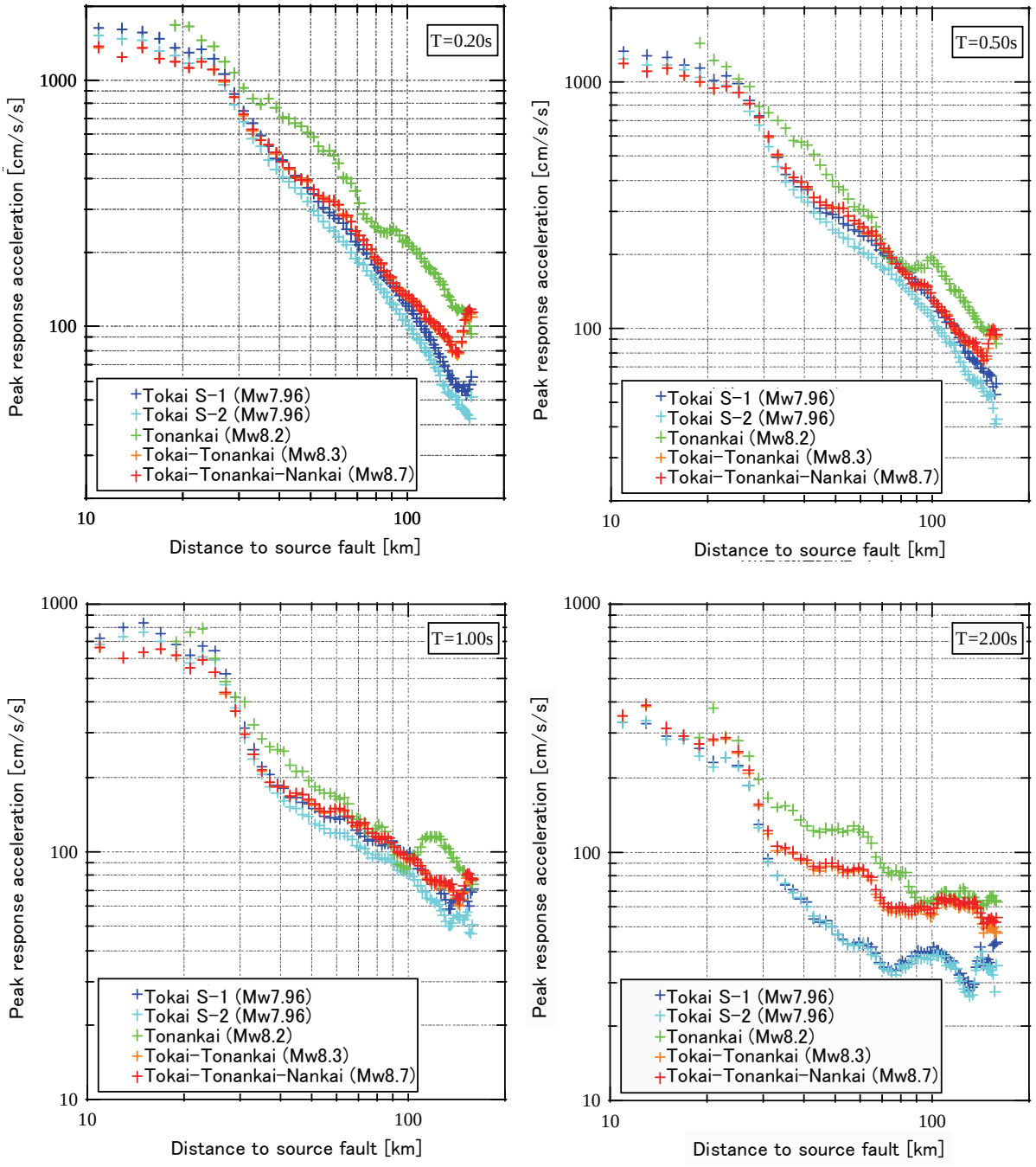

Fig. 8 Attenuation relationships of SA(T) of the ground motion during the Tokai, Tonankai, and Nankai earthquakes estimated by the Central Disaster Prevention Council.

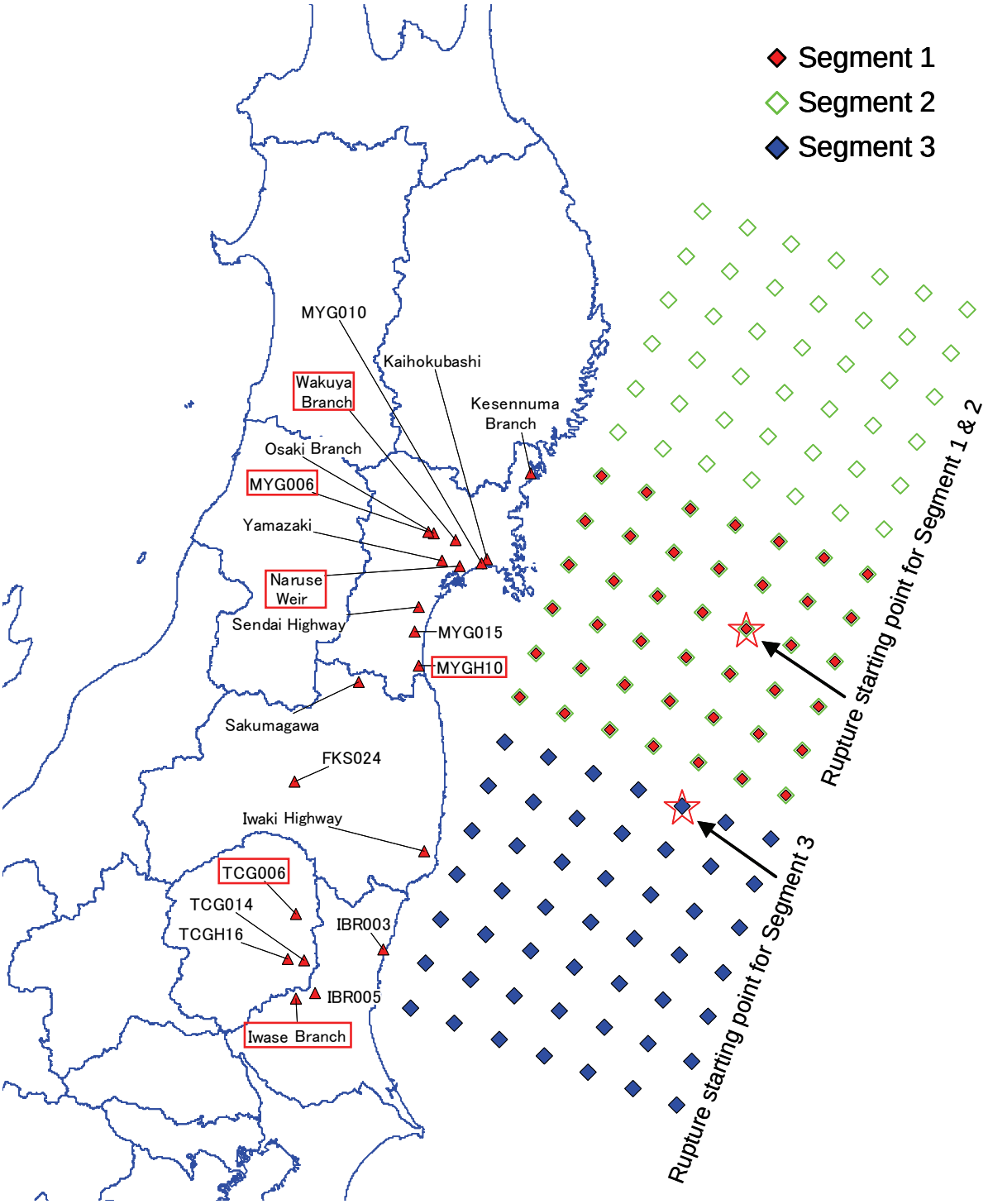

Fig. 9 The 3-Segment source fault used in the ground motion simulation. Point sources are located with interval of 25 [km]. The estimated ground motions at highlighted stations are shown in Fig. 10. Moment magnitudes are 8.48, 8.78, and 8.56 and rupture starting times are 0, 40, 100 [s] for Segments 1, 2, and 3, respectively.

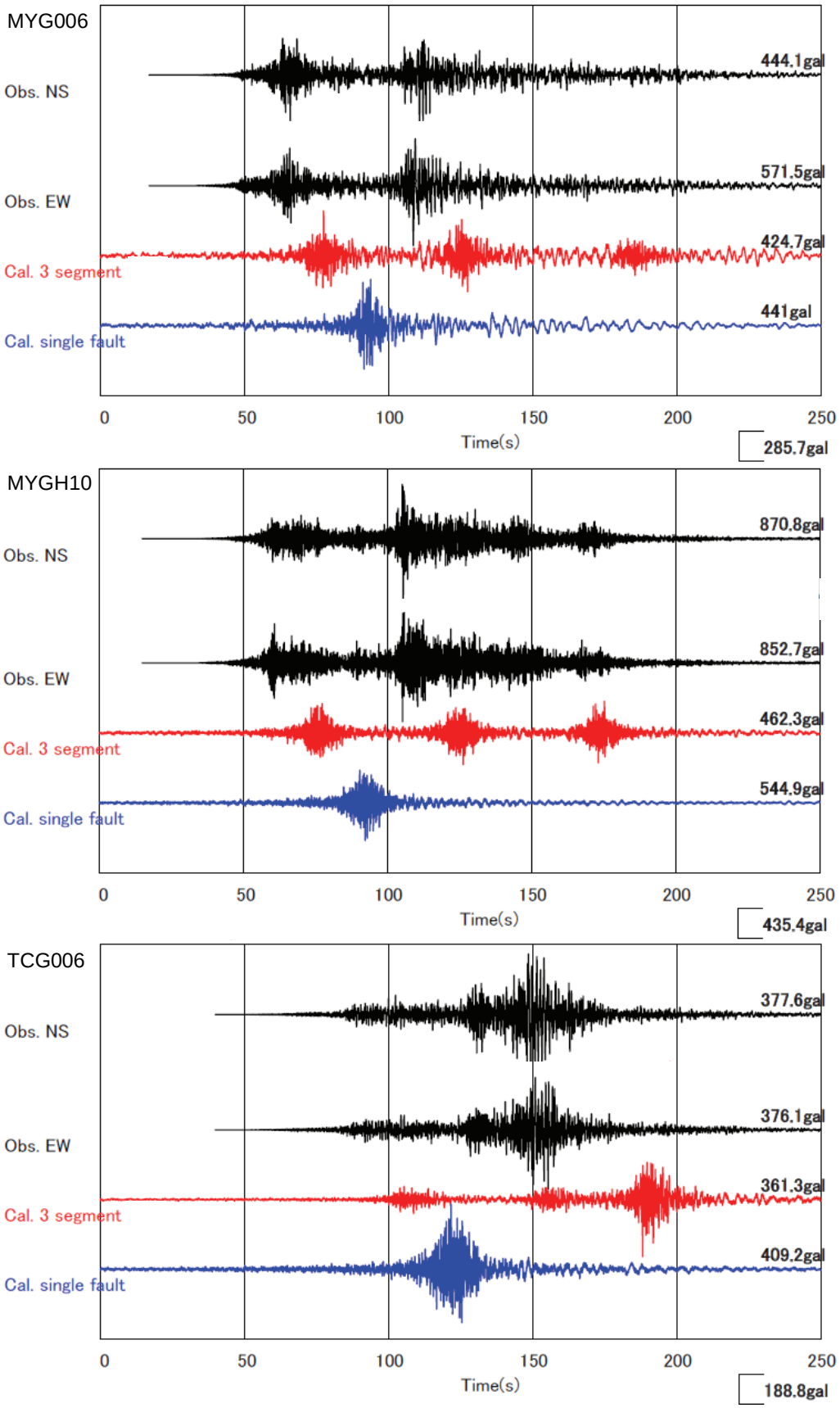

Fig. 10 Comparisons of time history waveforms of observed and estimated ground motions at MYG006, MYGH10, and TCG006.

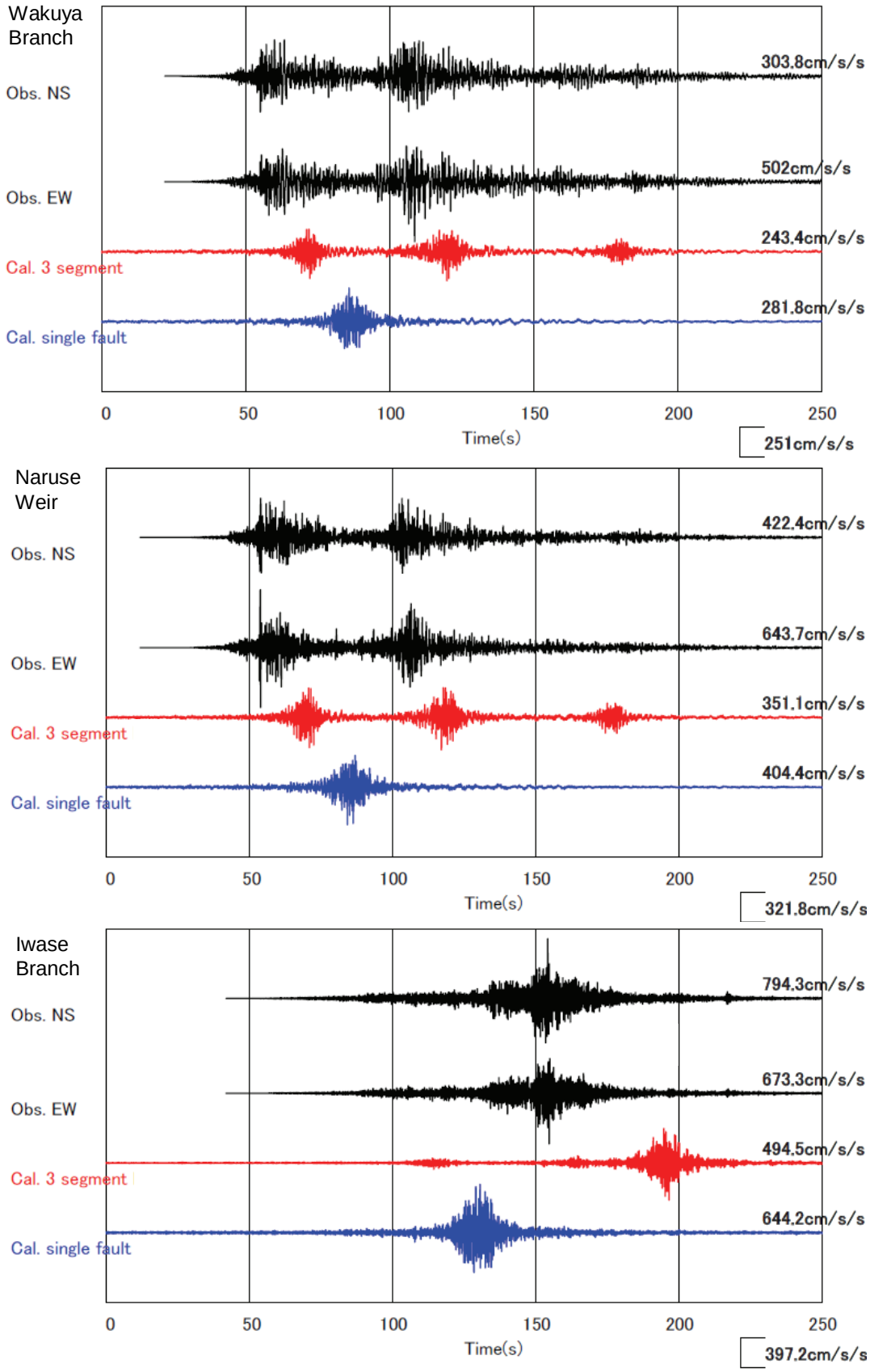

Fig. 11 Comparisons of time history waveforms of observed and estimated ground motions at Wakuya Branch, Naruse Weir, and Iwase Branch.

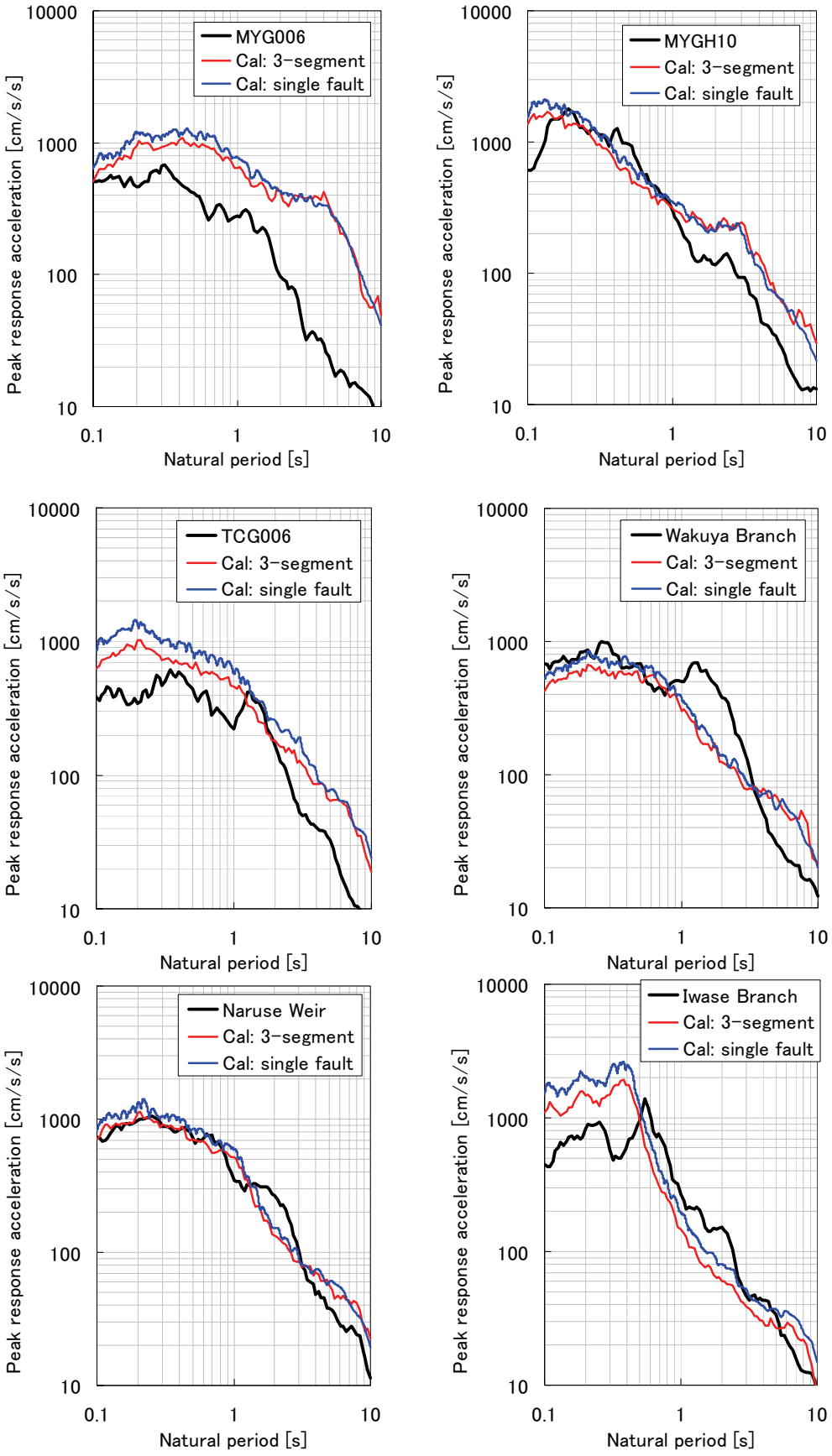

Fig. 12 Comparisons of acceleration response spectra of observed and estimated ground motions.